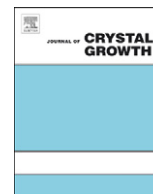




ELSEVIER

Contents lists available at SciVerse ScienceDirect

Journal of Crystal Growth

journal homepage: www.elsevier.com/locate/jcrysgr

Vectorial nanowire growth by local kinetic manipulation

Geunhee Lee^{a,1,*}, Yun Sung Woo^a, Jee-Eun Yang^a, Gil-Sung Kim^a, Donghun Lee^a, Kibum Kang^a, Cheol-Joo Kim^a, Moon-Ho Jo^{b,2,**}^a Department of Materials Science and Engineering, Pohang University of Science and Technology (POSTECH), San 31, Hyoja-Dong, Nam Gu, Pohang, Gyungbuk 790-784, Republic of Korea^b Department of Materials Science and Engineering, Yonsei University, 120-749 Korea, Seoul, Seodaemun-Gu, Seonsan-No 262

ARTICLE INFO

Article history:

Received 28 July 2011

Received in revised form

13 January 2012

Accepted 27 January 2012

Communicated by J.M. Redwing

Available online 4 February 2012

Keywords:

A1. Nanostructure

A2. Vectorial growth

B1. Nanowire

B2. Silicon

ABSTRACT

We report the vectorially controlled and well-aligned Si nanowires (SiNWs) array with enhanced optical absorption property in large area grown by the vapor–liquid–solid (VLS) mechanism as controlling the temperature gradient (TG) on the growth substrate. We demonstrate that the growth direction and magnitude of the SiNWs are quantitatively controllable in parallel and proportional to the locally imposed TG. We also show explicit examples of the vectorially controlled 3-dimensional NW growth on contoured or patterned substrates in the presence of the TG. The aligned SiNWs array shows excellent optical absorbance over a broad range of wavelength of 350–750 nm, which provides a practical implication of the well-ordered SiNWs system.

© 2012 Elsevier B.V. All rights reserved.

1. Introduction

Self-organized ensemble formation in nature is often found during the crystal growth at the various length scales, as in the prominent examples of block-copolymers, colloidal crystals, and solidification of alloys [1,2]. The integrated nanowire (NW) ensemble, which can serve as a common ground for the various applications into electronic circuits, biological probes, and energy conversion vehicles [3–7], requires such spontaneous ordering over a large anisotropic energy barrier set at the different length scales in the NW axial and radial directions. The vapor–liquid–solid (VLS) NW growth, which is the earliest and prevailing synthetic route for semiconductor NWs, typically employs the eutectic liquid catalysts of the nanometer size for the catalytic decomposition of the vapor precursors, the dimensionally confined nucleation and the subsequent one-dimensional growth [8–10]. Therein the crystallographic orientation of a NW is thermodynamically determined at the L–S interface within the eutectic liquid droplet of given size and

geometry during the initial nucleation [11,12]. Nevertheless, the embryonic NWs nucleate in an isotropically random manner at the edges of the hemispheric droplets [13,14], leading to an unpredictable growth unless the external constraints are imposed such as directional epitaxy or guiding templates [12,15]. Consequently, the systematic integration of VLS NWs usually requires supplementary processes posterior to the NW growth [16,17]. The VLS NW growth occurs in spatially uniform heating zones surrounding the growing crystals on substrates, thus all the reactions for the NW growth at the V–L–S phase boundaries are isothermal as illustrated in Fig. 1(a). The thermodynamic driving force for the VLS growth is the differences in the chemical potentials of the growth species, and they are uniformly distributed along the interfaces at the nanometer scale, through which the growth species are diffusively incorporated [18]. In principle, however, any local variation in the interfacial thermodynamics, i.e. local temperatures at the interfaces, can influence the elemental growth behaviors. In this aspect, we have earlier reported a simple and robust integrated growth scheme of SiNWs on the flat Si substrates along the temperature gradient (TG) in the anisothermal condition [19], as depicted in Fig. 1(b). We also provided a phenomenological model for the directional NW growth within the framework of the interfacial thermodynamic stability, particularly around the roles of the TG to redistribute the local kinetic variable on the thermodynamic stability at the fluctuating growth interfaces as schematically depicted in Fig. 1(c) [10].

Here, we demonstrate that this NW growth is spontaneous vectorial [19,20], i.e. both of the NW growth direction and

* Corresponding author. Tel.: +1 630 252 4080.

** Corresponding author at: Department of Materials Science and Engineering and Graduate Institute of Advanced Materials Science, Pohang University of Science and Technology (POSTECH), San 31, Hyoja-Dong, Nam Gu, Pohang, Gyungbuk 790-784, Republic of Korea.

E-mail addresses: glee@anl.gov (G. Lee), mhjo@postech.ac.kr (M.-H. Jo).¹ Present address: Materials Science Division, Argonne National Laboratory, 9700S. Cass Avenue., Argonne, IL 60439, US² Tel.: +82 54 279 2158; fax: +82 54 279 2399.

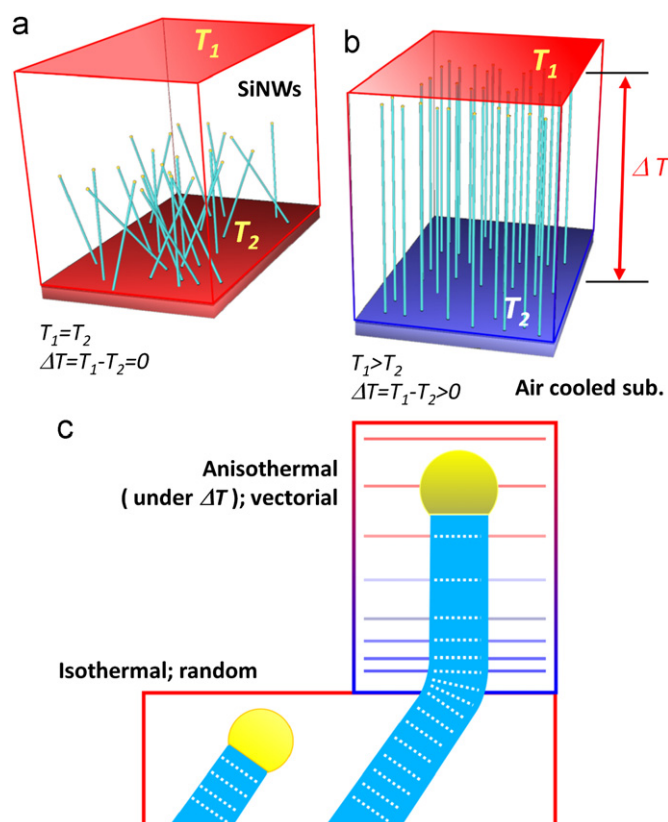


Fig. 1. Illustrations of (a) the conventional isothermal VLS growth, (b) the anisothermal VLS growth in our study, and (c) magnified schematics of the isothermal and anisothermal nanowire growth.

magnitude are proportional to the locally established TG, and are readily controllable and reproducible during the VLS growth in large area over $\sim 1 \text{ cm}^2$ regardless of shape of a substrate. We observe this growth scheme can be extended to achieve 3-dimensional NW assemblies on arbitrarily contoured or patterned substrates. In addition, the vectorially well-aligned Si NWs array showed excellent optical antireflection and absorption property over a broad range of wavelengths of 350–750 nm with a practical implication for the well-ordered NWs system.

2. Experiments

The NW growth was carried out in a quartz tube reactor of 2 in. in diameter, surrounded by a uniformly heating zone, with the susceptor underneath the growth substrates that can be cooled by air-circulation [19]. When the furnace was heating the reactor at 650°C , the temperature near the substrate was stably measured to be 490°C under air-circulation. Using 10% SiH_4 premixed in He of a total pressure of 50 Torr at the 50 sccm the typical NW growth was performed upon the nanoclusters of Au catalysts prepared by deposition of 2 nm thick Au films on 300 nm thick SiO_2/Si (100) substrate. We estimated the temperature distribution and its gradient in our CVD reactor under the identical experimental condition by computing the steady state thermal conduction, precisely described in our previous work [19].

3. Results and discussion

The grown SiNWs have tapered core-shell structure, i.e. single crystalline Si core with [112] or [111] crystalline-oriented growth

direction corresponding to their diameter of 50–80 nm and amorphous Si shell with several tens to hundreds nanometer in thickness [11,19] at the initially grown part. Fig. 2(a) demonstrates that the NW growth is directionally normal to the planar substrate and its directionality is reversibly achieved by the presence of the TG which is set linearly normal to the substrate over the planar region—note that the correspondingly simulated temperature and its TG are superimposed in Fig. 2(a). Specifically, upon the continuous NW growth, the linear TG is intermittently removed three times within a short interval of 90 s after growth of 6 min, 5 min, and 5 min by depleting the vapor precursor, resulting as marked by three horizontal dashed lines in Fig. 2(b). The vertical NW growth is correspondingly reproduced after the complicated kink formation (Fig. 2(c)) [19,21]. It should be also noted that the axial NW growth rate in each growth segment ($\Delta v = \Delta l/t$) is progressively reduced, as in Fig. 2(d), from 23.2 to $10.8 \mu\text{m}/\text{min}$ with decreasing the magnitude of the TG, when the NW growth front is farther away from the cold substrate. For qualitative comparison, we calculated the TG distribution along the surface-normal direction with corresponding boundary conditions whose magnitude linearly decreases from 382 to $346 \text{ K}/\text{cm}$ at the position indicated by blue vertical arrow in Fig. 2(a), and found a reasonable agreement, as in Fig. 2(e). With all aforementioned, the magnitude and the direction of the growth velocity of NWs, \vec{v} , linearly follow the ∇T , that implies the NW growth is vectorially controllable in local temperature gradient.

We also explored the observed vectorial growth scheme up on a contoured or patterned Si substrates with the presence of the TG, as seen in Fig. 3. We prepared trenched (001) Si substrates by area-selectively anisotropic chemical etching, as shown in the inset of Fig. 3(b). The general tendency was found that SiNWs were vertically grown very uniformly on the trenched substrate, as seen in Fig. 3(a) and (b). With closer observation in Fig. 3(b), we observed that SiNWs display certain characteristics in their directionality over the edges formed by two different sloped surfaces on a substrate, as depicted with yellow arrows: they are slightly deflected with respect to the surface-normal directions. We compute the TG distribution in the given geometry and the representative directions and magnitudes at each location as blue streamlines and red arrows, in the inset of Fig. 3(b). There is a remarkable similarity between the experimental and the calculated result for the specific NW directionality at each location as our expectation. In addition, we attempted to coherently direct the NW growth on selectively patterned substrates of a $500 \mu\text{m} \times 500 \mu\text{m}$ square shown in the inset of Fig. 3(c), formed by selective catalyst-deposition. As seen in Fig. 3(c) and (d), which is a magnified view of the lower and upper rectangle region of the inset, respectively, we obtained selectively and vertically well-aligned SiNWs in the pattern at a high density over $\sim 10^5 \text{ ea}/\text{mm}^2$ ($0.1 \text{ ea}/\mu\text{m}^2$) with uniform length.

We measured and compared the optical properties, i.e. the diffuse reflectance and absorbance of a bare (001) Si wafer, a randomly grown SiNWs on 300 nm thick SiO_2/Si (100) substrate, and the vectorially aligned SiNWs array on 300 nm thick SiO_2/Si (100) substrate, as shown in Fig. 4(a)–(c) and illustrated in Fig. 4(d), measured by an integrated sphere detector. The vectorially well-ordered SiNWs array was synthesized under the aforementioned TG condition for 10 min. The random SiNWs was formed under near isothermal condition of 490°C with the same growth time of 10 min. Because the growth rate under TG is much higher than that grown in the isothermal condition [19], there must be length difference in between each sample. The total length of SiNWs grown at 490°C and under TG for the same growth time of 10 min is around $30 \mu\text{m}$ and $120 \mu\text{m}$, respectively. The randomly grown SiNWs have a yellowish (or green) appearance in Fig. 4(b), showing that a large fraction of incident light is

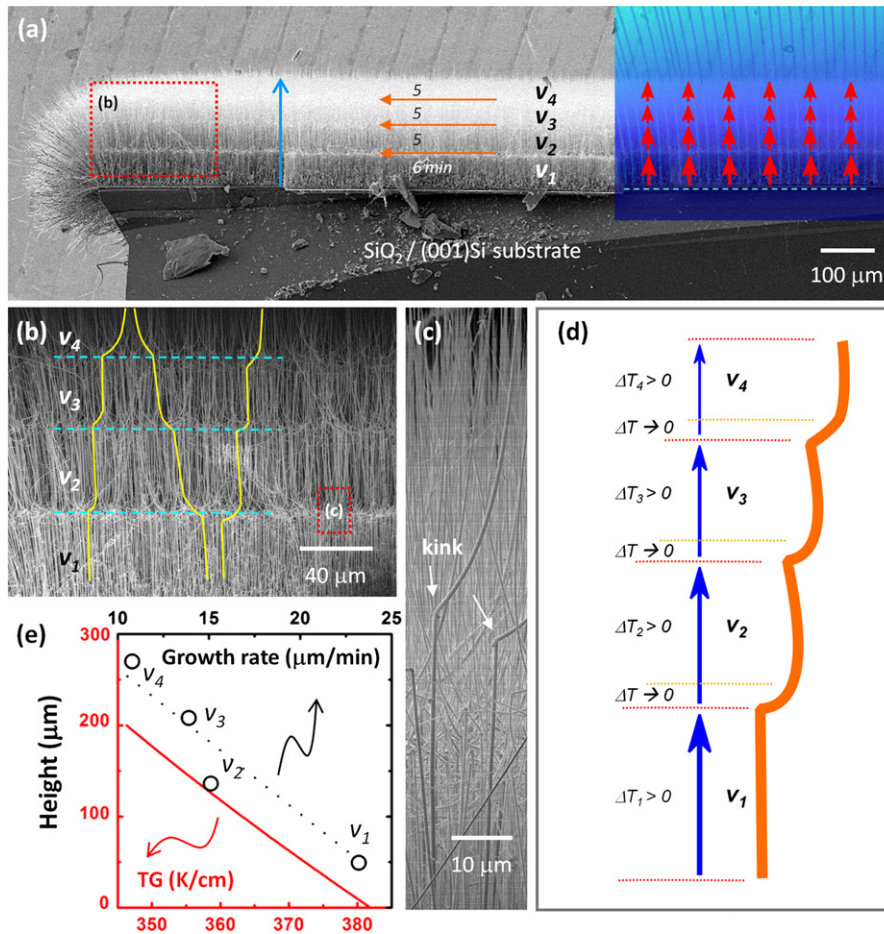


Fig. 2. (a) A cross-sectional SEM image of Si NWs on the flat 300 nm $\text{SiO}_2/(001)\text{Si}$ substrate (inset is the simulated the temperature (filled color) and its gradient (red arrows)), (b) the magnified red rectangular region in (a), (c) the magnified kinked Si NWs taken from the red rectangular region in (b), (d) schematic of the variation of the temperature gradient and growth rate for single Si NW, and (e) the calculated temperature gradient distribution (solid red line) taken from the location indicated by vertical blue arrow in (a), and the measured growth rate (open circle) with its linear fit (dot line). (For interpretation of the references to color in this figure legend, the reader is referred to the web version of this article.)

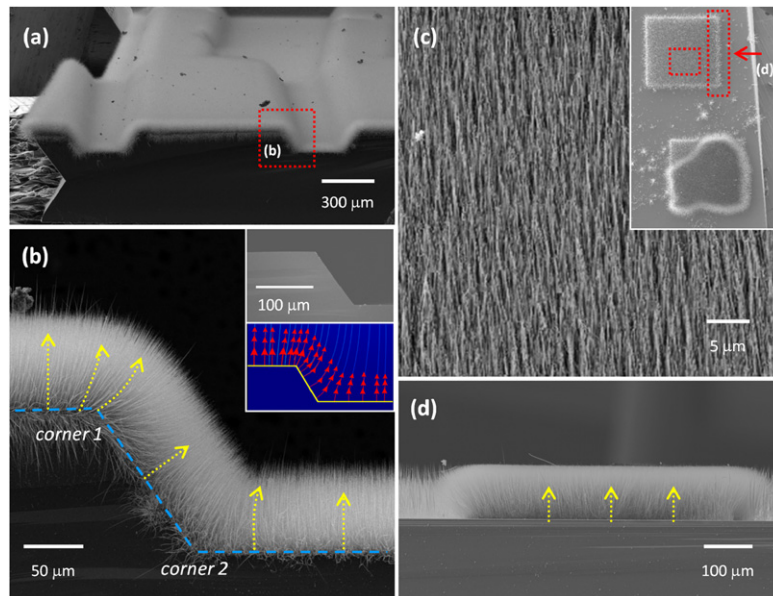


Fig. 3. (a) Macroscopic SEM image of the SiNWs on the patterned (001) Si surface, (b) the magnified red rectangular region in (a) (the insets are the bare patterned substrate (upper) and the simulated distribution of temperature and its gradient on the patterned substrates (lower)), (c) the tilt (15°) view of the vertically well-aligned SiNWs on the selectively patterned substrate (the inset is a macroscopic SEM image containing two patterns. The pattern area is defined as 500 $\mu\text{m} \times 500 \mu\text{m}$), and (d) the magnified side-view of the SiNWs indicated as side rectangular region of the inset of (c). (For interpretation of the references to color in this figure legend, the reader is referred to the web version of this article.)

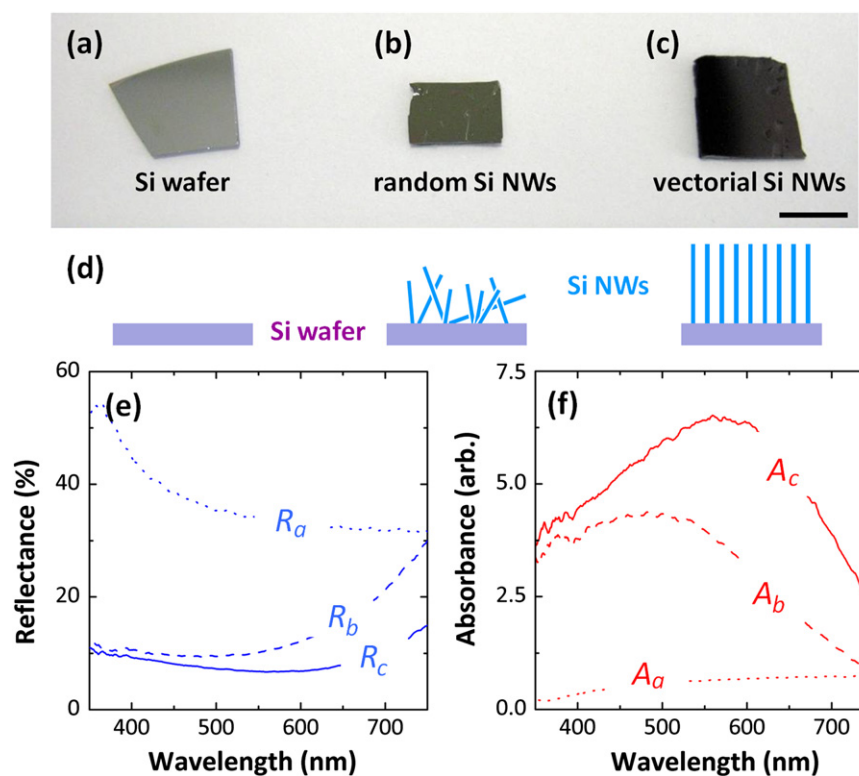


Fig. 4. Macroscopic images of (a) a bare (001) Si wafer (dotted line), (b) a randomly grown SiNWs array (dashed line), (c) a vectorially grown SiNWs array (solid line), (d) illustrated surface states, (e) optical diffuse reflectance, and (f) absorbance of each sample from (a) to (c). (For interpretation of the references to color in this figure, the reader is referred to the web version of this article.)

reflected by multiple scattering [22,23]. This yellow coloration implies relatively high absorption in the blue region of the visible spectrum as would be expected for silicon as dashed red line in Fig. 4(f). The reflection behavior of our random SiNWs is very similar with others reported one [22,23]. On the other hand, the vectorial SiNWs array shows lower reflectance in the whole wavelength range of 350–750 nm, where much of the solar flux in incident, of ~20% of bare Si wafer or ~60% of the randomly grown SiNWs. As a result, the well-aligned SiNWs array shows higher absorption of visible light in the whole wavelength range with the maximum absorption wavelength around 580 nm than the randomly grown SiNWs with maximum of 490 nm, which shows evidently enhanced optical absorption in the whole and specifically long wavelength region [24]. In addition, an effective impedance matching due to the cone shape of NWs from high homogenous decomposition and side wall deposition of Si during the growth [19], resulting in crystalline core and thick amorphous shell structure can affect the high absorbance and low reflectance [19,22,25]. Macroscopically, the aligned SiNWs array has a matte finish and is significantly darker (almost black) in appearance compared to the others (Fig. 4(c)). This excellent antireflection and absorption property could have promising approach for the optical or photo-energy applications of the massively integrated SiNWs array [24].

4. Conclusion

We demonstrate the vectorially controlled growth of SiNWs array in large area with enhanced optical absorbance in broad wavelength

range and extend the growth scheme for the 3-dimensional NWs assemblies upon the local and temporal TG manipulation, with practical implications.

Acknowledgments

This work was supported by the Basic Research Programs through the NRF (2009-0074051) and the WCU program through the MEST (R31-2008-000-10059-0).

References

- [1] G.M. Whitesides, B. Grzybowski, *Science* 295 (2002) 2418.
- [2] J.S. Langer, *Reviews of Modern Physics* 52 (1980) 1.
- [3] W. Lu, C.M. Lieber, *Nature Materials* 6 (2007) 841.
- [4] F. Patolsky, B.P. Timko, G. Zheng, C.M. Lieber, *MRS Bulletin* 32 (2007) 142.
- [5] C.K. Chan, H. Peng, G. Liu, K. McClwrath, X.F. Zhang, R.A. Huggins, Y. Cui, *Nature Nanotechnology* 3 (2008) 31.
- [6] B. Tian, X. Zheng, T.J. Kempa, Y. Fang, N. Yu, G. Yu, J. Huang, C.M. Lieber, *Nature* 885 (2007) 449.
- [7] M. Law, L.E. Greene, J.C. Johnson, R. Saykally, P. Yang, *Nature Materials* 4 (2005) 455.
- [8] R.S. Wagner, W.C. Ellis, *Applied Physics Letters* 4 (1964) 89.
- [9] A.M. Morales, C.M. Lieber, *Science* 279 (1998) 208.
- [10] S. Kodambaka, J. Tersoff, M.C. Reuter, F.M. Ross, *Physical Review Letters* 96 (2006) 096105; C.-B. Jin, J.-E. Yang, M.-H. Jo, *Applied Physics Letters* 88 (2006) 193105; J.-E. Yang, C.-B. Jin, C.-J. Kim, M.-H. Jo, *Nano Letters* 6 (2006) 2679.
- [11] Y. Wu, Y. Cui, L. Huynh, C.J. Barrelet, D.C. Bell, C.M. Lieber, *Nano Letters* 4 (2004) 433.
- [12] V. Schmidt, S. Senz, U. Gösele, *Nano Letters* 5 (2005) 931.
- [13] B.J. Kim, J. Tersoff, S. Kodambaka, M.C. Reuter, E.A. Stach, F.M. Ross, *Science* 322 (2008) 1070.
- [14] Y. Wu, P. Yang, *Journal of the American Chemical Society* 123 (2001) 3165.
- [15] C.-J. Kim, D. Lee, H.-S. Lee, G. Lee, G.-S. Kim, M.-H. Jo, *Applied Physics Letters* 94 (2009) 173105.
- [16] Y. Huang, X. Duan, Q. Wei, C.M. Lieber, *Science* 291 (2001) 630; D. Whang, S. Jin, Y. Wu, C.M. Lieber, *Nano Letters* 3 (2003) 1255;

- A. Javey, S. Nam, R.S. Friedman, H. Yan, C.M. Lieber, *Nano Letters* 7 (2007) 773.
- [17] J.-H. Ahn, H.-S. Kim, K.J. Lee, S. Jeon, S.J. Kang, Y. Sun, R.G. Nuzzo, J.A. Rogers, *Science* 314 (2006) 1754.
- [18] B.A. Wacaser, K.A. Dick, J. Johansson, M.T. Borgström, K. Deppert, L. Samuelson, *Advanced Materials* 20 (2009) 153.
- [19] G. Lee, Y.S. Woo, J.-E. Yang, D. Lee, C.-J. Kim, M.-H. Jo, *Angewandte Chemie International Edition* 48 (2009) 7366.
- [20] E. Joselevich, C.M. Lieber, *Nano Letters* 2 (2002) 1137.
- [21] R.S. Wagner, C.J. Doherty, *Journal of Electrochemical Society* 113 (1966) 1300; B. Tian, P. Xie, T.J. Kempa, D.C. Bell, C.M. Lieber, *Nature Nanotechnology* 4 (2009) 824.
- [22] R.A. Street, P. Qi, R. Lujan, W.S. Wong, *Applied Physics Letters* 93 (2008) 163109.
- [23] R.A. Street, W.S. Wong, C. Paulson, *Nano Letters* 9 (2009) 3494.
- [24] K. Peng, Y. Xu, Y. Wu, Y. Yan, S.-T. Lee, J. Zhu, *Small* 1 (2005) 1062.
- [25] J. Zhu, Z. Yu, G.F. Burkhard, C.-M. Hsu, S.T. Connor, Y. Xu, Q. Wang, M. McGehee, S. Fan, Y. Cui, *Nano Letters* 9 (2009) 279.